

Temporal Expression of Chitinase-like 3 in Wounded Murine Skin

Takehiko Murase^a, Takuma Yamamoto^a, Aki Koide^a, Yoichi Yagi^{a, b}, Shinichiro Kagawa^{a, b}, Shinichiro Tsuruya^{a, b}, Yuki Abe^a, Takahiro Umehara^a and Kazuya Ikematsu^a

^a: Division of Forensic Pathology and Science, Unit of Social Medicine, Graduate School of Biomedical Sciences, Nagasaki University School of Medicine

^b: Forensic Science Laboratory, Nagasaki Prefectural Police Headquarters

Correspondence should be addressed to: Takehiko Murase

Division of Forensic Pathology and Science, Unit of Social Medicine, Course of Medical and Dental Sciences, Graduate School of Biomedical Sciences, Nagasaki University School of Medicine, Nagasaki City, Nagasaki 852-8523, Japan

Tel.: +81-95-819-7076

Fax: +81-95-819-7078

E-mail: muras.bec.t@gmail.com

Keywords

Chitinase-like 3, Proteome, Skin, Mouse

Acknowledgement

We thank Dr. Okamoto and Prof., Dr. Morita, the Department of Virology, Institute of Tropical Medicine, Nagasaki University. We also thank the staff of the Biomedical Research Center, Division of Comparative Medicine, Center for Frontier Life Sciences, Nagasaki University.

This work was supported by Japan Society for the Promotion of Science (KAKENHI Grant Number 23590853).

Abstract

In forensic practice, it is important to diagnose wound age accurately. We analyzed the proteome of injured murine skin to identify a novel protein marker of wound age after recent injury. We used samples from 3 days after injury, with 0 days as the control. The proteins were separated with two-dimensional electrophoresis. Using mass spectrometry, we identified a protein, chitinase-like 3 (Chil3). Chil3 mRNA expression showed temporal changes, which included a peak increase at 2 days after injury. Next, we produced an anti-Chil3 antibody and confirmed its specificity with western blotting. Similar to the mRNA results, an analysis of temporal changes in Chil3 protein expression revealed a peak at 2 days after injury. We also investigated the time-course of changes in Chil3 tissue localization using immunohistochemistry. Chil3 signals remained in the wounded area for up to 9 days. However, Chil3-positive cells were observed in the scab, the edge of the dermal layer and neogenetic granulation tissue between 1 and 3 days. Thus, wound age can be histologically determined using the localization of Chil3 but not its general existence. Additionally, double-labeled fluorescent immunohistochemistry revealed that the Chil3-expressing cells were mainly neutrophils. These data show that Chil3 is expressed in neutrophils during the early stage of wound healing in mice; thus, Chil3 is a potential histological marker of 1-3-day-old wounds.

1 Introduction

Forensic pathologists are required to diagnose the age of wounds during autopsies. Macromorphology of wounds (e.g., color changes of subcutaneous hemorrhages and scabbing) provide primary information, however, it is unsuitable for the accurate determination of wound age from only it.

Wound repair mechanisms are divided into three stages based on pathophysiological aspects; inflammation, proliferation, and maturation [1-3]. Histopathological examinations are typically used to determine the chronological order of changes that occur during each stage, including the conventional hematoxylin-eosin (HE) staining and/or Prussian blue staining [4-6]. HE staining is an essential method of visualizing cytomorphology, however, identifying the types of cells those infiltrate wounds during healing requires proficiency for forensic pathologists. Prussian blue staining is frequently used for age estimations. The limitation with this method is that positive staining requires a wound age of 5-7 days. Therefore, Prussian blue staining cannot detect the very early stages of wound healing.

Various cells and biomolecules play a role in wound repair, and many pathologists speculated that some of these markers could be used to determine wound age based on their fluctuations during tissue repair [7]. Pathologists have estimated earlier wound ages by measuring the levels of enzymes and/or bioactive substances, such as ATPase, phosphatase, serotonin, and histamine [7-10]. To date, a large number of

studies have investigated wound age estimation using collagen, cytokines, adhesion molecules and/or their combinations as indicator [11-24].

Hence, the development of a useful method to accurately determine wound age at early stages is essential; therefore, we completed the following study; first, we determined the time-course of mRNA and protein expression for the identified compounds after the proteome analysis. Next, we assessed the specific protein localization and temporal expression of the potential protein marker using histological methods with murine injured skin. We report that the utility of the protein chitinase-like 3 (Chil3) was examined for wound age determination.

2 Materials and methods

2.1 Animal Experiments

2.1.1 Animal model

Pathogen-free 6-week-old male BALB/cCrSlc mice were obtained from SLC, Inc. (Shizuoka, Japan). As previously described, skin wounds were created in mice [25, 26]. Briefly, mice were anesthetized by an intraperitoneal injection of sodium pentobarbital (50 mg/kg). After shaving to remove the fur, six full-thickness excisional wounds were created on the dorsal skin using a 4-mm biopsy punch (Kai medical,

Tokyo, Japan). After the procedure, each mouse was housed in a sterilized cage and provided autoclaved food and redistilled water to prevent bacterial infections. The mice were euthanized at 1, 2, 3, 5, 7, and 9 days after injury. Mice euthanized on 0 days served as a control. The Animal Care Committee of Nagasaki University approved our research protocol (Approved No. 1410211181-2).

2.1.2 Biochemistry

The dorsal skin of euthanized mice was exfoliated and excised around the wound edges with a 6-mm biopsy punch (Kai Medical). For protein examination, the tissue samples were frozen in liquid nitrogen and preserved at -80 °C until use. For RNA analysis, the tissue samples were immersed in RNAlater® (Life Technologies, Carlsbad, CA, USA) overnight at 4 °C and then preserved at -80 °C.

2.1.3 Histology

After euthanasia, samples immediately underwent perfusion fixation with phosphate-buffered 4% paraformaldehyde (PFA, Wako, Tokyo, Japan). The dorsal injured skin was exfoliated and fixed overnight with phosphate-buffered 4% PFA in 4 °C. For immunohistochemistry (IHC), fixed skin samples were cut, dehydrated, paraffinized, and embedded. The paraffin blocks were preserved in the dark at room

temperature. For fluorescent IHC (fIHC), fixed skin samples were cryoprotected with 10 and 20% sucrose solutions. The samples were cut and embedded in O.C.T compound (Bright Cryo-M-Bed; Bright instruments, Huntingdon, UK) on dry ice and preserved at -80 °C.

2.2 Two-dimensional electrophoresis (2-DE)

2.2.1 Sample preparation for protein analysis

Each 10-mg skin specimen with a zirconia bead (Nikkato Corporation, Osaka, Japan) and 400µL of protein extract solution was homogenized twice using a Tissue Lyser (Qiagen, Hilden, Germany) at 25 Hz for 30 sec. The lysed tissue and buffer was centrifuged (15000 × g, 30 min, 4 °C). The protein concentration of the supernatant was measured using the RC DC™ protein assay kit (Bio-Rad Laboratories, Hercules, CA, USA). The protein extraction solution contained 8 M urea (Wako), 2 M thiourea (Wako), 3% CHAPS (Dojindo, Kumamoto, Japan), 1% Triton X-100 (Wako), 50 mM dithiothreitol (DTT, Nakalai Tesque, Kyoto, Japan), and 1% Biolyte® pH 3.5-10 (Bio-Rad Laboratories).

2.2.2 2-DE

The steps for 2-DE were performed in accordance with the Isoelectric Focusing System User's Manual (Anatech, Tokyo, Japan) and previously reported method [27]. An immobilized pH gradient (IPG) ReadyStrip™ (Bio-Rad Laboratories, pH 4-7, 18 cm) was used for the first dimension. The strips were rehydrated overnight in the protein extraction solution with 0.0025% orange G. Next, 50 µg of protein was added to the cathode end of each strip, and the strips were run from 500 to 3,000 V in stages for 8 hrs and then run at 3500 V for 10 hrs at 20 °C. The strips were subsequently treated for protein reduction and alkylation. The reduction solution contained 6 M urea, 50 mM DTT, 25 mM Tris-HCl (pH = 8.8), 2% sodium dodecyl sulfate (SDS, Wako), and 30% glycerol (Wako). The alkylation solution contained 6 M urea, 80 mM iodoacetamide (IAA, Nakalai Tesque), 25 mM Tris-HCl (pH = 8.8), 2% SDS, and 30% glycerol. Next, the strips were applied to vertical homogeneous acrylamide 12%T gels and run using the SDS-discontinuous system (20 mA/gel, 15 °C).

2.2.3 Image acquisition and statistical analysis

Proteins in the gels were visualized using a Silver Stain Plus™ Kit (Bio-Rad Laboratories) according to manufacturer's instructions. The stained gels were scanned with an Image Scanner (GE Healthcare UK Ltd., Little Chalfont, Buckinghamshire, England) and LabScan Software (GE Healthcare) and saved as 16-bit

TIFF images. The images were analyzed with Shimadzu Phoretix™ 2D Expression ver. 2005 (Shimadzu Corporation, Kyoto, Japan) using the default analysis wizard and evaluated for differences between injured skin and the control. An un-paired t-test was used for statistical analysis. A p-value of less than 0.05 indicated a statistically significant difference.

2.3 Mass Spectrometry

2.3.1 Sample preparation and analysis

In-gel digestion was performed in accordance with previously reported method [27]. The silver-stained spots were cut into 1-mm³ pieces and destained with 15 mM potassium ferricyanide (Wako) /50 mM sodium thiosulfate (Wako). After washing the gels with redistilled water and 50 and 100% acetonitrile (AcCN, Wako), the proteins were reduced with 10 mM DTT and alkylated with 50 mM IAA. The gels were equilibrated and dehydrated with 50 mM ammonium bicarbonate (NH₄HCO₃, Wako), 50% AcCN/50mM NH₄HCO₃, and 100% AcCN. Next, the gels were incubated with a trypsin (Wako) solution at 37 °C overnight in NH₄HCO₃ buffer. The digested peptides were extracted from the gels with 0.3% formic acid. The extract solutions were used for liquid chromatography-tandem mass spectrometry (LC-MS/MS) analysis.

2.3.2 LC-MS/MS

The LC-MS/MS method was performed as previously described [28]. MS and tandem-MS spectra were obtained using an LC-electrospray ionization-linear ion trap-q-time of flight (LC-ESI-LIT-q-TOF) spectrometer (NanoFrontier eLD, Hitachi High-technologies, Tokyo, Japan). A peptide extract solution was used, and peptides were trapped by C18 column (MONOLITH TRAP C18-50-150, Hitachi High-technologies). Peptide separation was completed with a packed nano-capillary column (NTCC-360/75-3, Nikkyo Technos, Tokyo, Japan) at a flow rate of 200 nL/min. The peptides were eluted using a stepwise acetonitrile gradient (Buffer A: 2% acetonitrile/0.1% formic acid, Buffer B: 98% Acetonitrile/0.1% formic acid, Gradient protocol: 0 min A = 100% B = 0%, 60 min A = 0%, B = 100%). The separated peptides were ionized with a capillary voltage of 1700 V. The ionized peptides were detected with a detector potential TOF range of 2050-2150 V. The raw data were converted into the Mascot format using data processing software (Hitachi High-Technologies) and analyzed using the MASCOT database (Matrix Science Inc., Boston, MA, USA).

2.4 Analysis of mRNA expression

Skin samples of 10 mg in RNAlater® were used for the RNA analysis. The total RNA was extracted, reverse transcribed, and subjected to quantitative real-time polymerase chain reaction (PCR) following previously published methods [25,29]. The primers for Chil3 mRNA and ribosomal protein S18 mRNA (Rps18), which served as an internal control, were purchased from Takara Bio Inc. (Ootsu, Japan). Statistically significant differences were assessed, and Steel's multiple-comparison test was applied for post hoc analysis using R ver. 3.3.1 [30]. A p-value less than 0.05 indicated a statistically significant difference.

2.5 Analysis of identified protein expression

2.5.1 Development of a specific antibody

We requested Scrum Inc. (Tokyo, Japan) to create a specific antibody against Chil3. According to their reports, the short peptide chain of Chil3 (amino acids 287-299 C+STGPPGKYTDESG) was synthesized. Next, a mixture of the peptide conjugated with KLH and Freund's complete adjuvant was injected five times in rabbits, and the total blood was obtained 7 days after the last immunization. The peptide-specific antibodies were purified from sera using immunoaffinity chromatography.

2.5.2 Verification of antibody specificity

The proteins were extracted from 2-day-old injured skin with an extraction buffer containing 150 mM NaCl, 30 mM Tris, 3% CHAPS, 1% Triton X-100, and 50 mM DTT. The protein concentration of each supernatant was measured using an RC DC™ protein assay kit (Bio-Rad Laboratories). Next, the samples were separated on a 4-12% NuPAGE® Bis-Tris gel (Life Technologies) and transferred to a polyvinylidene fluoride membrane with an iBlot® Dry Blotting System (Life Technologies). We detected our protein of interest using pre-immunized serum and anti-Chil3 antibodies (α -Chil3) as the primary antibody with the Western Breeze® Chemiluminescent Kit (Life Technologies) according to the manufacturers' instructions. The serum and α -Chil3 were used at a 1:500 dilution. The luminescent band was imaged with LAS-3000 mini (Fuji Film, Tokyo, Japan).

We also performed an antigen absorption test to evaluate antibody specificity. Briefly, solutions containing α -Chil3 (1:500) were incubated with agarose media conjugated with the antigenic peptide. Unconjugated media was used as a control. After centrifugation, the supernatant was used for Western blotting (WB) as a primary antibody solution.

2.5.3 Determination of temporal protein expression using WB

Protein samples were chronologically collected from injured skin and control skin. These samples were then subjected to WB with α -Chil3 (1:500) and anti- β -tubulin (as an internal control, 1:1000) as the primary antibodies. Protein bands were visualized by chemiluminescence, and the band intensity was calculated using Quantity One® (Bio-Rad) as the ratio of Chil3/ β -tubulin. Statistical significance was assessed by Kruskal-Wallis test and Dunn's multiple comparison test using Graph-Pad Prism® ver. 5.0c. (GraphPad Software Inc.). A p-value less than 0.05 indicated a statistically significant difference.

2.6 Histology

2.6.1 Double-label fIHC

Double-label fIHC was performed with α -Chil3, anti-F4/80 (α -F4/80, macrophage marker), and anti-Ly-6G (α -Ly-6G, neutrophil marker) as primary antibodies in accordance with IHC and immunofluorescence (IF) protocols (Abcam). Rat anti-mouse F4/80 was purchased from Bio-Rad Laboratories, rat anti-mouse Ly-6G was purchased from Novus Biologicals (Littleton, CO, USA), and goat anti-rabbit IgG (H+L), Alexa Fluor® 488 conjugated (α -rabbit 488), and Alexa Fluor® 594 conjugated (α -rat 594) secondary antibodies were purchased from Life Technologies.

Specimens were sectioned with a thickness of 5 μm using a cryostat. After complete drying at RT, the sections were rehydrated and treated with a block solution (phosphate-buffered saline containing 1% casein, 5% normal goat serum, and 0.1% TritonX-100) for 1 h at RT. Next, the sections were incubated in a primary antibody solution (α -Chil3 and α -F4/80 in block solution, 1:200 and 1:100, respectively, or α -Chil3 and α -Ly-6G in block solution, 1:200 and 1:100, respectively) overnight at 4 °C. Samples were incubated in a secondary antibody solution (α -rabbit 488 and α -rat 594 in block solution, 1:500 for both antibodies) for 1 h at RT. The sections were mounted with VECTASHIELD Mounting Medium with DAPI (VECTOR Laboratories).

2.6.2 IHC

We used a chronological set of injury and control samples for IHC. The paraffinized specimens were sectioned at a thickness of 5 μm with a microtome. IHC was performed with α -Chil3 as the primary antibody using standard IHC protocols (Abcam, Cambridge, UK). After heat-mediated antigen retrieval with citrate buffer (pH = 6.0), sections were treated with a block solution (tris-buffered saline containing 1% Casein, 5% normal horse serum, and 0.1% Triton-X 100) for 1 h at room temperature. The sections were incubated in a primary antibody solution (α -Chil3 in block solution, 1:200) overnight at 4 °C. Next,

samples were incubated with ImmPRESS™-Alkaline Phosphatase Polymer Anti-Rabbit IgG Reagent (VECTOR Laboratories, Burlingame, CA, USA) for 1 h at room temperature. The Histofine® fast red II substrate kit (Nichirei Bioscience Inc., Tokyo, Japan) was used as a color developer. Hematoxylin was used as a nuclear counterstain.

2.6.3 Observation and assessment

We used a BZ-9000 (Keyence, Osaka, Japan) for microscopic observations. The obtained images were processed with analysis software (Keyence).

3 Results

3.1 2-DE and protein identification

We detected approximately 500 protein spots per gel in a pH range of 4-7 using silver staining (Supplemental Fig. S1). The statistical analysis revealed that the densities of only five spots showed a reliable increase when compared with the control. We used LC-MS/MS to identify the proteins within these five spots. However, only two proteins were identified: Chil3 and NHL repeat-containing 2 (NHLrc2). We

were unable to identify the three remaining spots. Representative images of the Chil3 spot are shown in Fig.

1a. The density comparisons between 0 and 3 days are shown in Fig. 1b.

3.2 mRNA expression

RT-PCR was performed to examine changes in the mRNA expression of Chil3 and NHLrc2. The level of Chil3 mRNA increased from 1 day, drastically peaked by 2 days, and then progressively decreased until returning to baseline at 7 days. There were significant differences between 2 days after injury and 0, 5, 7, and 9 days after injury (Fig. 2). NHLrc2 mRNA did not show significant changes (data not shown).

3.3 Antibody examination

To evaluate antibody specificity, WB was performed with 2-day-old wound samples (Supplemental Fig. S2). We detected multiple bands with diluted pre-immunized serum as the primary antibody. A single band was detected at approximately 45 kDa with an immunoaffinity-purified antibody. This band was not identified in the blot that was incubated with pre-immunized serum. The antigen absorption test revealed no signal was identified with the solution treated with antigen-conjugated media. A single band using the antibody solution treated with unconjugated media (data not shown).

3.4 Protein expression

The quantification of temporal changes in Chil3 protein expression showed a pattern similar to our mRNA results. The representative WB image of the temporal changes in Chil3 expression is shown in Fig. 3a. Chil3 protein increased from 1 day and showed an approximately 500-fold peak increase on 2 days. The protein levels then progressively decreased until 9 days after injury. Statistically significant differences were found between 2 days and 0, 7, 9 days (Fig. 3b).

3.5 Histological examinations

3.5.1 Double-label fIHC

We performed double-label fIHC on samples collected in 2 days after injury. We observed Chil3- and F4/80-positive cells, and these cells contained oval nuclei (Fig. 4a). The Chil3 signal was small and granular in cytoplasm (Fig. 4a, arrows). A several portion of F4/80-positive cells was negative for Chil3. On the other hand, we found the cells that possessed the stronger signals than that of macrophages (Fig. 4a, arrowheads). In addition, we identified Chil3 and Ly-6G double-positive cells at the wound site (Fig. 4b).

Chil3 signal was granular and homogeneous in the cytoplasm, and these cells had polymorphous nuclei.

Nearly all of the Ly-6G-positive cells were also positive for Chil3.

3.5.2 Chil3 expression within wounds

We found Chil3-positive cells in 2-day-old wound (Fig. 5a). Two types of positive cell were identified. One was small and oval type (Fig. 5a, arrows), and the other was large and elongated (Fig. 5a, arrowheads). In addition, Chil3-positive cells were detected between 1 and 9 days after injury (Fig. 5b), whereas positive cells were rarely detected in control samples. On 1 day, positive cells appeared in the scab, the edge of the dermal layer and the neogenetic granulation tissue around the wound. The positive cells remained in these areas during 2-3 days. Positive cells were localized to the residual scab and the surface of the granulation tissue between 5 and 9 days. There was no signal at the edge of the normal tissue and a large part of the granulation tissue.

4 Discussions

In this study, we used samples from the early stages of wound repair. The early wound stage, especially 3 days after injury, presents the peak of the inflammatory period, characterized by an increase of activated

immune cells [1-3], providing an ideal condition for the detection of biological markers representing the drastic changes at the site of wound.

Although there are various analytical methods for the detection of biomolecules, a comprehensive analysis is needed for the wide range of cells and biomolecules involved in wound healing. Furthermore, a suitable marker must have sufficient stability against degradation because of its forensic application [31]. In this case, a protein marker would be far superior to an mRNA marker. To complete our comprehensive protein analysis, we employed 2-DE to assess protein dynamics. We detected approximately 500 spots with 2-DE; however, only five spots were significantly different between 0 and 3 days of injury. The limited detection of significant differences may be due to the use of a silver stain, which has a narrow dynamic range and poor protein visualization [32]. Subsequent proteome analysis identified only 2 out of the above-mentioned 5 spots: NHLrc2 and Chil3. In general, silver stain tends to overestimate the amount of protein in gels; thus, there may be an insufficient amount of protein for identification despite the clear detection of the spot [32]. NHLrc2 mRNA expression did not show a temporal pattern; therefore, we did not analyze this protein further. Our gel analysis may have detected post-translational modifications (PTMs) including phosphorylation and/or glycosylation, rather than an increase in transcription.

Qualitative changes, such as PTMs, may be useful for wound age estimation. Therefore, a further analysis of NHLrc2 expression during wound healing is warranted.

Chil3, also known as Ym1, is a murine protein [33]. Macrophages, dendritic cells, and mast cells are considered to major producers of Chil3. It shares significant structural similarity to family 18 chitinases. It is a functional marker of alternatively activated macrophages, which exert anti-inflammatory effects, promote wound healing, and combat parasitic infections; however, the role of Chil3 in healing and phylaxis remains unclear. While some chitinase and chitinase-like protein are lost their function of chitin breakdown, they have binding-activity to carbohydrates and matrix and might contribute to matrix reorganization and wound healing [34].

In this study, Chil3 mRNA and protein were drastically increased from 1 to 3 days after injury, and it was suggested that Chil3 expressed cells were two types in 2 days after injury. Our results indicated that Chil3 might have some functions during the early period of wound healing. As described above, several studies have suggested that Chil3 is generally expressed by alternatively activated macrophages, which may control inflammation in wounds and enhance healing [35-40]. We confirmed that macrophages around wound expressed Chil3 with our results of fIHC, and assumed that Chil3 positive macrophages might have

some roles described above in wound. However, we found the cells that had stronger signals than macrophage. These cells might play a major role of Chil3 expression.

On the other hand, Goren et al. reported that neutrophils had Chil3 mRNA expressions and Chil3 was mainly expressed in neutrophils rather than macrophages in wound healing [41]. In addition, Harbord et al. demonstrated that Chil3 presented in neutrophil and macrophage, and neutrophil showed higher concentration than macrophage [42]. We also found neutrophil and macrophage expressed Chil3 from the results of IHC and fIHC. In addition, we considered that neutrophil strongly expressed it from the results of fIHC. These findings corresponded to their reports. Generally, regarding the transition of inflammatory cells in wounds, neutrophils are dominant up to 2-3 days after injury, whereas macrophage numbers gradually increase and peak at 3-5 days [3,43]. In this study, we revealed that Chil3 mRNA and protein was increased in wounds, particularly 2 days after injury. The period of Chil3 expression was similar to the neutrophil dominant phase in wound healing. This coincidence supported that Chil3 is mainly expressed in neutrophils during the early stages of wound repair. Therefore, we regarded neutrophil as a primary Chil3 expresser.

Although mRNA might detect wound age more sensitively than protein, mRNA is easily degraded [31]. Thus, protein analyses are more appropriate in the forensics field. Based on standard forensic

practices, an IHC investigation is required. To accommodate the potential impact of this limitation on novel biomarkers, we utilized paraffin-embedded sections for histological examination. Chil3 signals were hardly detected on 0 days. This result suggests that Chil3 is not produced by intact skin. Indeed, the Chil3 signal appeared in the scab and the edge of the dermal layer 1 day post-injury. The signal continued to increase during 2-3 days at the aforementioned sites and in neogenetic tissue. In contrast, the Chil3 signal was found only in the residual scab and at the surface of the granulation tissue on 5-9 days. We confirmed that the Chil3 signal existed at the edge of the normal tissue and neogenetic granulation tissue until 3 days, and the signal disappeared from the site after 5 days. Thus, 1-3-day-old wounds might be determined by the localization of Chil3.

Adhesion molecules, cytokines and collagens were advocated as wound age marker [2,6]. Some adhesion molecules (e.g. fibronectin, selectins and cell adhesion molecules) and some cytokines (e.g. interleukin-1, interleukin-6 and tumor necrosis factor- α) indicated the wound after several tens of minutes or hours from injury. Some collagens were detected with several days or a week-old wound. Compared with them, Chil3 had a different time-specificity and could find the wound age during 1 to 3 days in our murine model. Therefore, Chil3 might be useful for wound age estimation. We certainly realized that multiple detection of wound age marker must be suitable for highly-detailed investigation. However, even

if multiple markers such as cytokines and collagens are used, the wound age estimation is still vague and very difficult in forensic practice. We have impression that application of our results might slightly contribute to diagnose wound age estimation.

Although we had not investigated human samples yet, we have plan to examine the protein expression in human, such as Chitinase, Acidic (CHIA), which is homolog of the protein for human, and Chitinase 3 like 1 (CHI3L1) and Chitinase 1 (CHIT1, Chitotriosidase) that have highly-matched sequence to it.

In conclusion, our results suggest that Chil3 is markedly expressed by neutrophils in injured skin, particularly during the inflammatory period. Thus, Chil3 is a candidate of marker for wound age estimation using immunohistochemical techniques. There are several proteins with sequences that highly match to Chil3, such as CHIA, CHI3L1 and CHIT in humans. Therefore, a further investigation concerning these proteins is needed to apply for wound age determination in forensic practice.

Disclosure of conflicts of interests

This study was supported by Japan Society for the Promotion of Science (KAKENHI Grant Number 23590853).

The authors declare no conflict of interest associated with this manuscript.

References

1. Martin P. (1997) Wound healing—aiming for perfect skin regeneration. *Science* 276:75–81
2. Kondo T., Ishida Y. (2010) Molecular pathology of wound healing. *Forensic Sci Int* 203:93–98
3. Broughton G., Janis J.E., Attinger C.E. (2006) The basic science of wound healing. *Plast Reconstr Surg* 117:12S–34S
4. Betz P. (1994) Histological and enzyme histochemical parameters for the age estimation of human skin wounds. *Int J Legal Med* 107:60–68
5. Betz P., Eisenmenger W. (1996) Morphometrical analysis of hemosiderin deposits in relation to wound age. *Int J Legal Med* 108: 262–264
6. Grellner W., Madea B. (2007) Demands on scientific studies: vitality of wounds and wound age estimation. *Forensic Sci Int* 165:150–154
7. Janssen W. (1984) *Forensic Histopathology*. Springer-Verlag
8. Raekallio J. (1970) Enzyme histochemistry of wound healing. *Prog Histochem Cyto* 1:III–I92
9. Raekallio J. (1972) Determination of the age of wounds by histochemical and biochemical methods. *Forensic Sci Int* 1:3–16

10. Dachun W., Jiazhen Z. (1992) Localization and quantification of the nonspecific esterase in injured skin for timing of wounds. *Forensic Sci Int* 53:203–213
11. Betz P., Nerlich A., Wilske J., Tübel J., Penning R., Eisenmenger W. (1993) Analysis of the immunohistochemical localization of collagen type III and V for the time-estimation of human skin wounds. *Int J Legal Med* 105:329–332
12. Betz P., Nerlich A., Wilske J., Tübel J., Penning R., Eisenmenger W. (1993) Immunohistochemical localization of collagen types I and VI in human skin wounds. *Int J Legal Med* 106:31–34
13. Dressler J., Bachmann L., Kasper M., Hauck J.G., Müller E. (1997) Time dependence of the expression of ICAM-1 (CD 54) in human skin wounds. *Int J Legal Med* 110:299–304
14. Dressler J., Bachmann L., Koch R., Müller E. (1998) Enhanced expression of selectins in human skin wounds. *Int J Legal Med* 112:39–44
15. Dressler J., Bachmann L., Koch R., Müller E. (1999) Estimation of wound age and VCAM-1 in human skin. *Int J Legal Med* 112:159–162
16. Kondo T., Ohshima T. (1996) The dynamics of inflammatory cytokines in the healing process of mouse skin wound: a preliminary study for possible wound age determination. *Int J Legal Med* 108:231–

17. Kondo T., Ohshima T., Eisenmenger W. (1999) Immunohistochemical and morphometrical study on the temporal expression of interleukin-1 α (IL-1 α) in human skin wounds for forensic wound age determination. *Int J Legal Med* 112:249–252
18. Kondo T., Ohshima T., Mori R., Guan D.W., Ohshima K., Eisenmenger W. (2002) Immunohistochemical detection of chemokines in human skin wounds and its application to wound age determination. *Int J Legal Med* 116:87–91
19. Guan D.W., Ohshima T., Kondo T. (2000) Immunohistochemical study on Fas and Fas ligand in skin wound healing. *Histochem J* 32:85–91
20. Kondo T., Tanaka J., Ishida Y., Mori R., Takayasu T., Ohshima T. (2002) Ubiquitin expression in skin wounds and its application to forensic wound age determination. *Int J Legal Med* 116:267–272
21. Hayashi T., Ishida Y., Kimura A., Takayasu T., Eisenmenger W., Kondo T. (2004) Forensic application of VEGF expression to skin wound age determination. *Int J Legal Med* 118:320–325
22. Kondo T. (2007) Timing of skin wounds. *Legal Med* 9:109–114
23. Takamiya M., Fujita S., Saigusa K., Aoki Y. (2008) Simultaneous detection of eight cytokines in human dermal wounds with a multiplex bead-based immunoassay for wound age estimation. *Int J Legal Med* 122:143–148

24. Cecchi R. (2010) Estimating wound age: looking into the future. *Int J Legal Med* 124:523–536
25. Kagawa S., Matsuo A., Yagi Y., Ikematsu K., Tsuda R., Nakasono I. (2009) The time-course analysis of gene expression during wound healing in mouse skin. *Legal Med* 11:70–75.
26. Yagi Y., Murase T., Kagawa S., Tsuruya S., Nakahara A., Yamamoto T., Umehara T., Ikematsu K. (2016) Immunohistochemical detection of CD14 and combined assessment with CD32B and CD68 for wound age estimation. *Forensic Sci Int* 262:113–120
27. Toda T. (1997) Standardization of protocol for Immobiline 2-D PAGE and construction of 2-D PAGE protein database on World Wide Web home page. *Jpn J Electroph* 41:13–19
28. Okamoto K., Endo Y., Inoue S., Nabeshima T., Nga P.T., Guillermo P.H., Yu F., Loan D.P., Trang B.M., Natividad F.F., Hasebe F., Morita K. (2010) Development of a rapid and comprehensive proteomics-based arboviruses detection system. *J Virol Methods* 167:31–36
29. Sakai S., Ikematsu K., Matsuo A., Tsai C.T., Nakasono I. (2010) Expression of C-fos, Fos-b, Fosl-1, Fosl-2, Dusp-1 and C-jun in the mouse heart after single and repeated chlorpromazine administrations. *Legal Med* 12:284–288
30. R Core Team (2016) R: A Language and Environment for Statistical Computing. R Foundation for Statistical Computing, Vienna, Austria <https://www.R-project.org/>

31. Inoue H., Kimura A., Tsuji T. (2002) Degradation profile of mRNA in a dead rat body: basic semi-quantification study. *Forensic Sci Int* 130:127–132
32. Twyman R. (2013) *Principles of Proteomics*. Garland Science
33. Gupta G. (2012) *Animal lectins: form, function and clinical applications*. Springer Science+Business Media
34. Tamás Rőszér (2015) Understanding the Mysterious M2 Macrophage through Activation Markers and Effector Mechanisms. *Mediat Inflamm* vol. 2015, Article ID 816460
35. Chang N.C., Hung S.I., Hwa K.Y., Kato I., Chen J.E., Liu C.H., Chang A.C. (2001) A macrophage protein, Ym1, transiently expressed during inflammation is a novel mammalian lectin. *J Biol Chem* 276:17,497–506
36. Mosser D.M., Edwards J.P. (2008) Exploring the full spectrum of macrophage activation. *Nat Rev Immunol* 8:958–969
37. Raes G., De Baetselier P., Noël W., Beschin A., Brombacher F., Hassanzadeh Gh. G. (2002) Differential expression of Fizz1 and Ym1 in alternatively versus classically activated macrophages. *J Leukocyte Biol* 71:597–602

38. Raes G., Van den Bergh R., De Baetselier P., Ghassabeh G.H., Scotton C., Locati M., Mantovani A., Sozzani S. (2005) Arginase-1 and Ym1 are markers for murine, but not human, alternatively activated myeloid cells. *J Immunol* 174:6551–6552
39. Welch J.S., Escoubet-Lozach L., Sykes D.B., Liddiard K., Greaves D.R., Glass C.K. (2002) Th2 cytokines and allergic challenge induce Ym1 expression in macrophages by a STAT6-dependent mechanism. *J Biol Chem* 277:42,821–42,829
40. Gordon S. (2003) Alternative activation of macrophages. *Nat Rev Immunol* 3:23–35
41. Goren I., Pfeilschifter J., Frank S. (2014) Uptake of neutrophil-derived Ym1 protein distinguishes wound macrophages in the absence of interleukin-4 signaling in murine wound healing. *Am J Pathol* 184:3249–3261
42. Harbord M., Novelli M., Canas B., Power D., Davis C., Godovac-Zimmermann J., Roes J., Segal A.W. (2002) Ym1 is a neutrophil granule protein that crystallizes in p47^{phox}-deficient mice. *J Biol Chem* 277:5468–5475
43. Witte M.B., Barbul A. (1997) General principles of wound healing. *Surg Clin N Am* 77:509–528

Captions of Figures

Fig. 1a Representative enlarged images of the Chil3 spot in 2-DE gels (arrows). (i) Sample of 0 days after injury and (ii) 3 days after injury

Fig. 1b Differences of Chil3 spot densities. Data are shown as the mean \pm SEM (n = 4). Statistical significance is indicated with an asterisk *; $p < 0.05$

Fig. 2 Time-course changes in Chil3 mRNA expression. Data are shown as the mean \pm SEM (n>5). Statistical significance is indicated with an asterisk *; $p < 0.05$

Fig. 3a Representative image of temporal changes of Chil3

Fig. 3b Temporal changes of Chil3 protein. Data are shown as the mean \pm SEM (n=4). Statistical significance is indicated with an asterisk *; $p < 0.05$

Fig. 4a Double-label fIHC with α -Chil3 and α -F4/80 in a 2-day-old wound. (i) Chil3, (ii) F4/80, (iii) DAPI and (iv) Merging, scale bar = 10 μ m

Fig. 4b Double-label fIHC with α -Chil3 and α -Ly-6G in a 2-day-old wound. (i) Chil3, (ii) Ly-6G, (iii) DAPI and (iv) Merging, scale bar = 10 μ m.

Fig. 5a (i) Representative image of immunohistochemistry with α -Chil3 antibody in 2 days-old wound,

scale bar = 50 μ m (ii) Enlarged image, scale bar = 10 μ m

Fig. 5b Temporal changes of Chil3 expression in skin wounds. (i) 0 days, (ii) 1 day, (iii) 2 days, (iv) 3

days, (v) 5 days, (vi) 7 days, and (vii) 9 days after injury, scale bar = 50 μ m

Fig. S1 Representative 2-DE images. (i) Sample of 0 days after injury (Control) and (ii) 3 days after

injury

Fig. S2 Antibody evaluation. Proteins extracted from samples collected 2 days after injury were used for

WB with (i) diluted pre-immunized serum, (ii) an antibody after immunoaffinity purification from

post-immunized serum, and (iii) an antibody after antigen absorption treatment

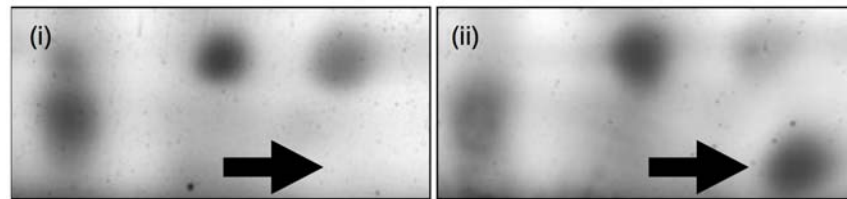


Fig. 1a

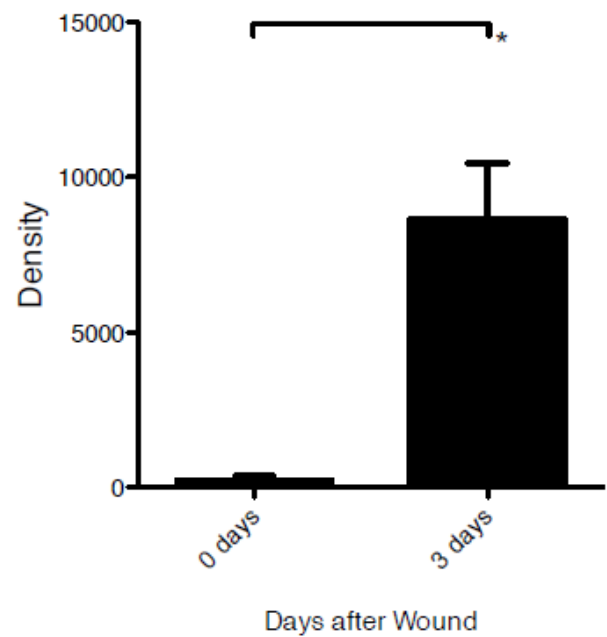


Fig.1b

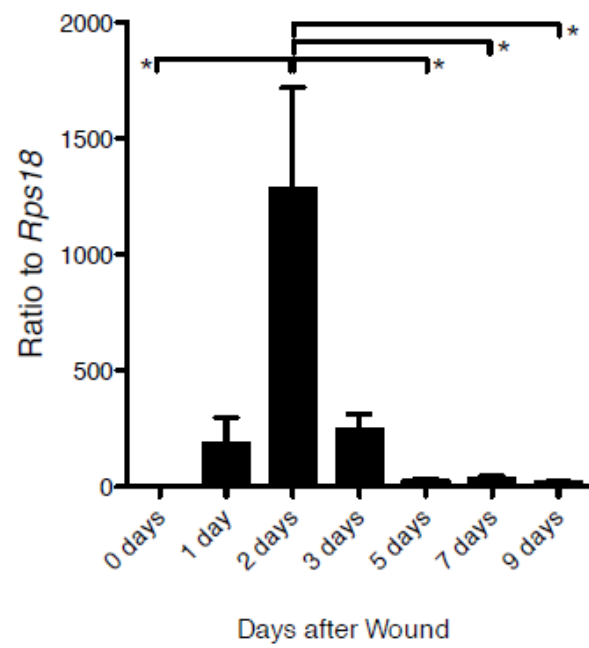


Fig. 2

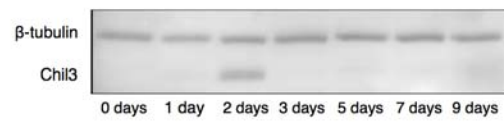


Fig. 3a

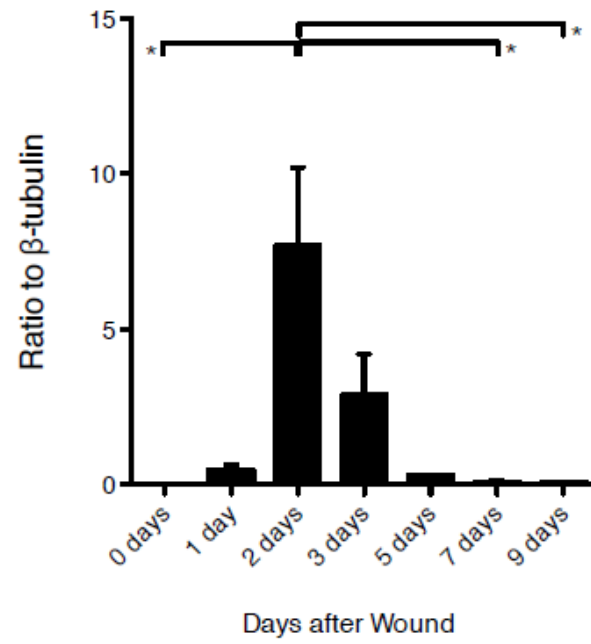


Fig. 3b

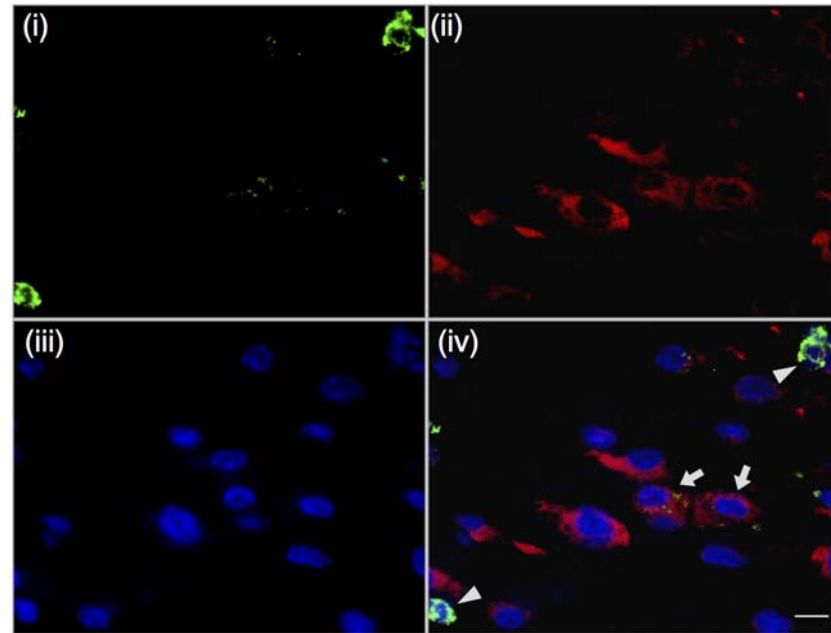


Fig. 4a

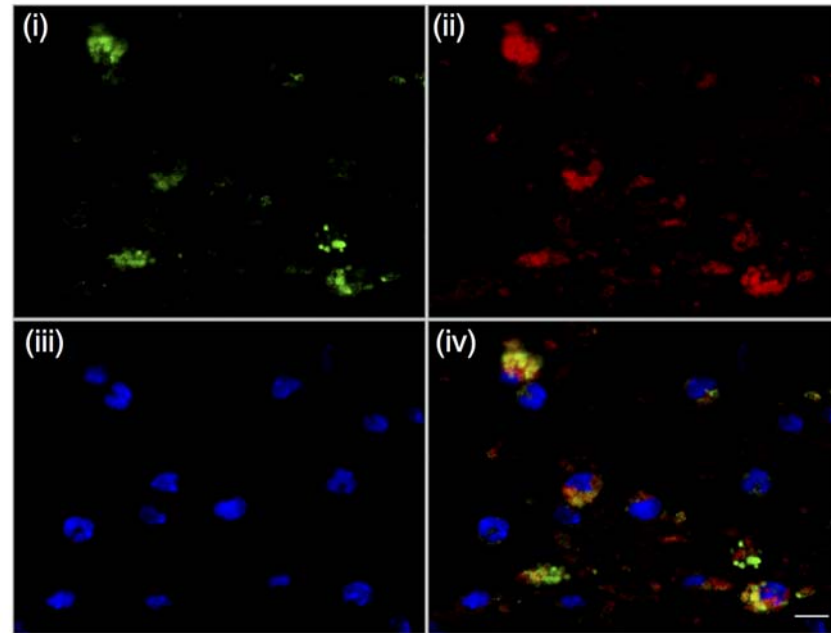


Fig. 4b

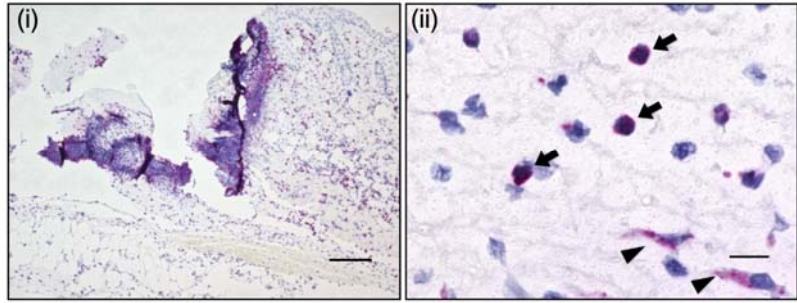


Fig. 5a

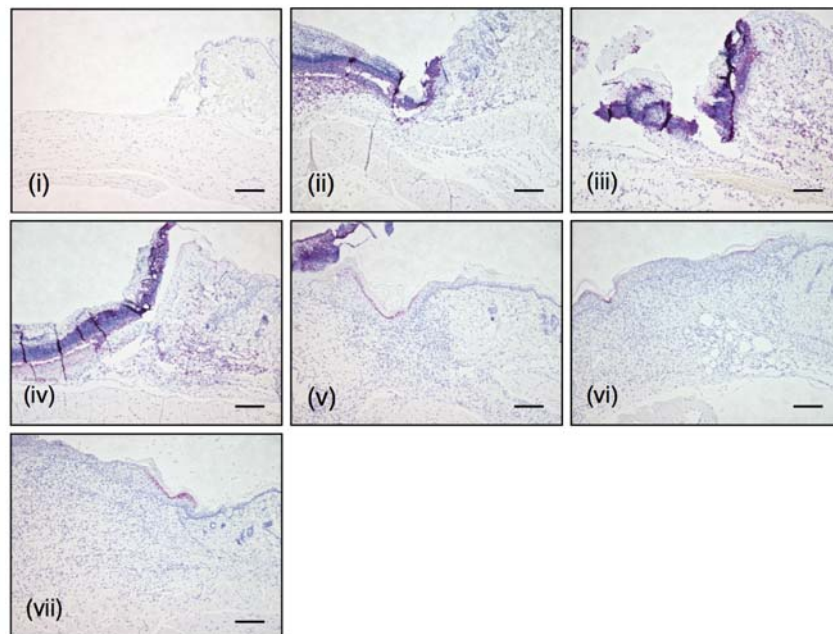


Fig. 5b

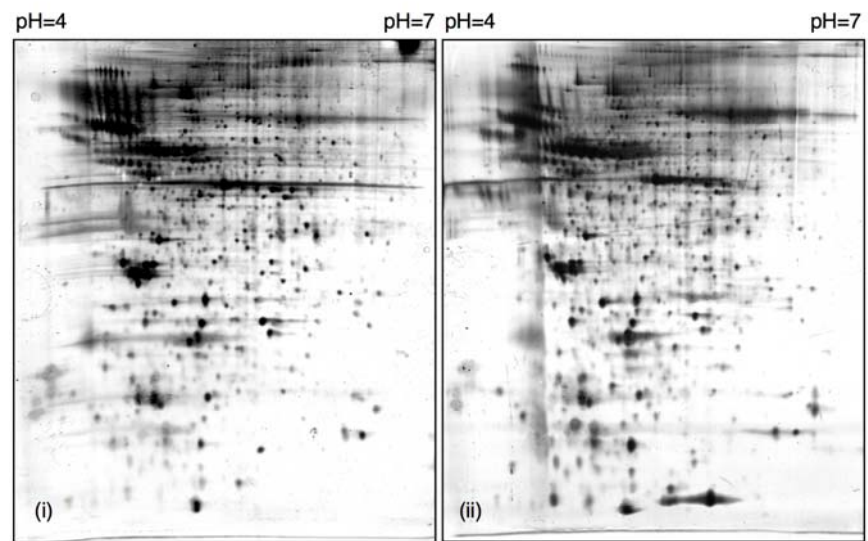


Fig. S1

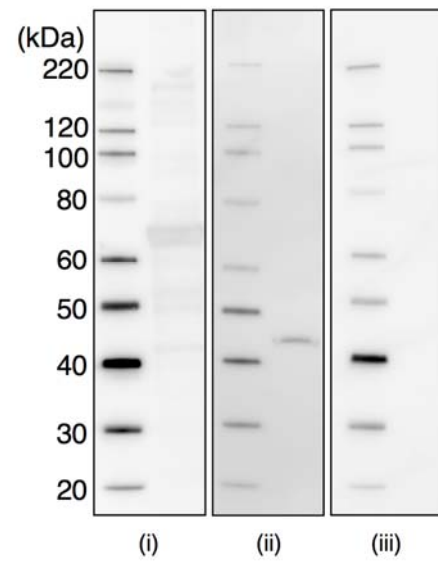


Fig. S2